Available online at www.sciencedirect.com
ScienceDirect
Cement and Concrete Research 37 (2007) 270–282
Cement and Concrete Research

A microstructural approach to adherence mechanism of poly (vinyl alcohol) modified cement systems to ceramic tiles

A.A.P. Mansur, D.B. Santos, H.S. Mansur *

Department of Metallurgical and Materials Engineering of Federal University of Minas Gerais, Rua Espírito Santo, 35/316-Centro. Belo Horizonte/MG, 30.160–030, Brazil

Received 29 March 2006; accepted 12 November 2006

Abstract

PVA is a water soluble polymer used as cement modifier. An important modification observed by addition of PVA is the increase of the bond strength between cement paste and aggregate. The purpose of this work was to investigate the effect of PVA on the mechanism of adherence of cement pastes to ceramic tiles. Pastes with and without PVA were applied on the back side of porcelain tiles and after 56 days the microstructures of the interfaces were evaluated by SEM. The mode of rupture changed from mostly interfacial failure to a mixed-mode interfacial-cohesive failure for the paste with polymer addition in which was observed the reduction of the thickness of the porous transition zone between tile and paste bulk. Also, in plain paste the formation of a duplex film (CH plus C–S–H) in contact with tile surface was observed while in modified paste a single layer of C–S–H was identified.

Keywords: Microstructure (B); SEM (B); Bond strength (C); Admixture (D); Interfacial transition zone (B)

1. Introduction

Poly(vinyl alcohol) (PVA or PVOH) is a water soluble polymer used as cement modifier [1]. PVA polymer is usually added in small amounts (up to 3 wt.% based on cement mass) as aqueous solutions to cement pastes, mortars and concretes [1–5].

PVA polymer is also present in latex polymeric mortars as stabilizer originating from emulsion polymerization and further added to the dispersion as a poly(vinyl alcohol)/anti-blocking agent (minerals) admixture for the spray drying of the dispersion [6,7]. At present, most of latexes used in mortar modification are generally commercially manufactured with the presence of up to 5% surfactants, including PVA, for latex stabilizations [8].

As general effects of PVA in cement based materials properties, improvement of workability and water retention are observed [1,2,4]. Some authors have noted a decrease of compressive strengths due to the increase of air voids content [2]. Others, however, have obtained improvement of compressive strength and reduction of porosity associated with interactions of PVA with fly ash blended cement, forming some new compounds that fill the pores or improve the bond between cement grains [3]. An important modification observed by addition of PVA is the significant increase of the bond strength between cement paste and aggregate changing the failure mode from an adhesive to cohesive [4].

The possibility of bonding improvement on the interface between ceramic tiles and modified mortars is crucial for the use of adhered method with modified cement mortars for installation of ceramic tiles. In the last years, around the world, the lack of confidence in ceramic tiles and mortar industry has raised with an overall result of reduction in the industry growth and, indirectly, it has an adverse impact upon all manufactures, merchants and installers [9–11]. Besides that, when evaluating ceramic tile systems failures, adhesive rupture between cladding and modified mortar was observed in 84% of the buildings [12]. This value was somehow expected because the modeling of ceramic tile coverings behavior reveals the highest shear stresses in tile/tile bed interface, when considering stresses caused by moisture expansion or thermal movements [13].

The purpose of this work was to investigate the effect of poly (vinyl alcohol) admixture on the mechanism of adherence of

* Corresponding author. Tel.: +55 31 32381843; fax: +55 31 32381815.
E-mail address: hmansur@demet.ufmg.br (H.S. Mansur).

0008-8846/$ - see front matter © 2006 Elsevier Ltd. All rights reserved.
doi:10.1016/j.cemconres.2006.11.011

Table 1
Typical properties of Portland cement CPII-F32 obtained from the producer

Chemical composition wt.%										
SiO_2	Al_2O_3	Fe_2O_3	CaO	MgO	SO_3	Na_2O	K_2O	CO_2	IR	LOI
17	5	3	60	6	3	<1	1	4	1	5

Physical properties						
Setting time (min)		# 200 (%)	Blaine Surface Area (m^2/kg)	Compressive strength (MPa)		
Initial	Final			3 days	7 days	28 days
275	345	3	338	28	31	39

cement pastes based on microstructural evaluation of cement pastes/porcelain ceramic tiles interface by scanning electron microscopy (SEM). Also, X-Ray Diffraction (XRD) and Fourier Transformed Infrared Spectroscopy (FTIR) analyses were conducted in order to evaluate the effect of the organic admixture in cement hydration.

2. Experimental procedure

2.1. Materials

Portland cement type CPII-F 32 according to Brazilian Standard NBR 11578/91 and deionized water were used to prepare the pastes.

The composition and properties of the cement are shown in Table 1, according to the manufacturer (Cimento Tupi, Brazil). The PVA used was Celvol 603 (Celanese Chemicals, USA), low molecular mass of 13,000–23,000 g/mol and was 81% hydrolyzed PVA.

The choice of this PVA among the wide spectrum of PVAs commercially available with different degrees of hydrolysis and chain lengths was supported by several features. In the literature concerned to PVA as a cement modifier [2,4,14] one can observe mostly the use of PVAs partially hydrolyzed, with degree of hydrolysis between 87–89%. When considering the studies of macro-defect free cements, [5,15–17] the investigations were

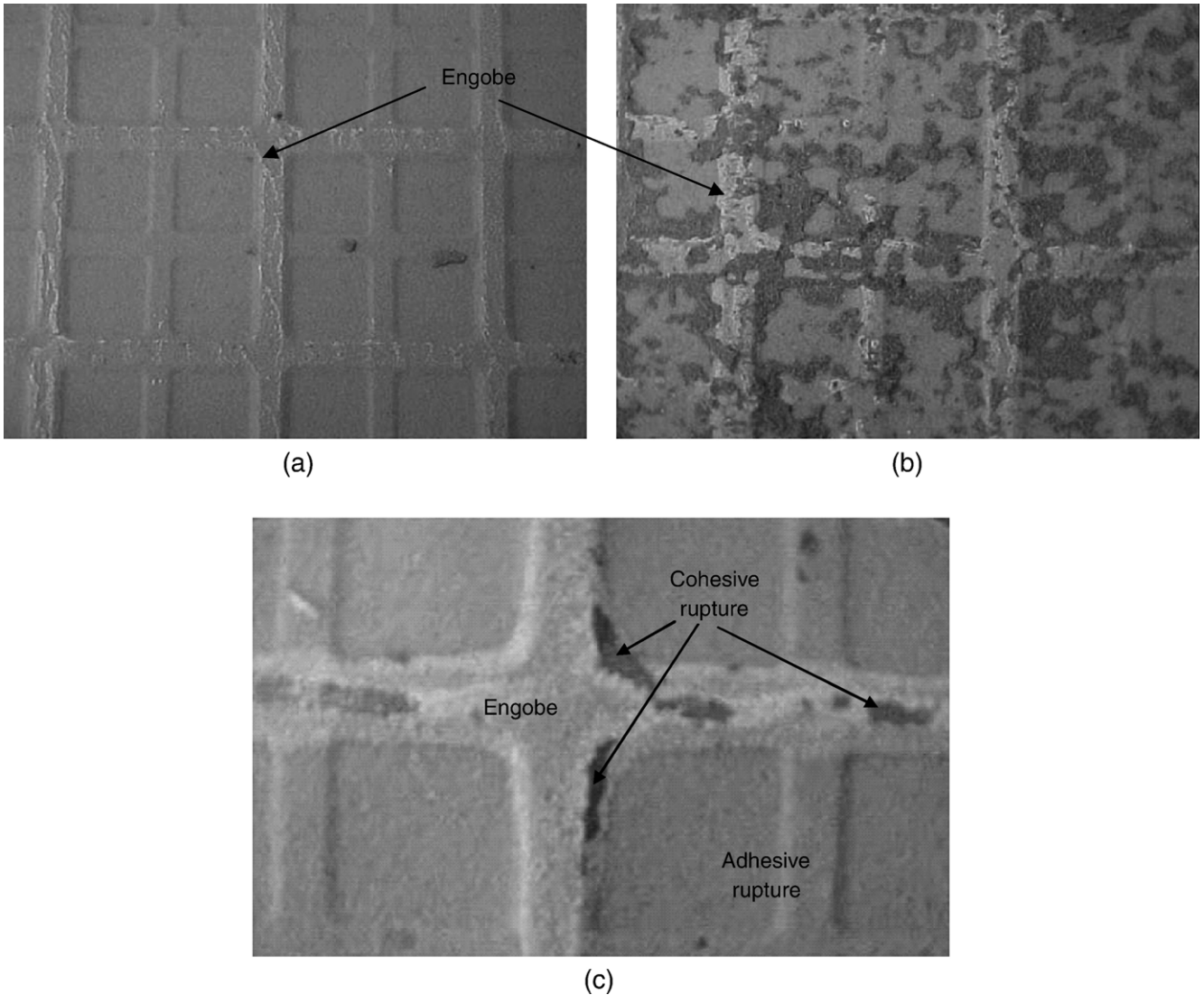

Fig. 1. Images acquired from failure surface on the tile side of (a) cement paste without PVA and (b) cement paste with 2.0 wt.% of PVA (polymer to cement ratio). The images reveal the presence of engobe that favors a cohesive rupture of unmodified cement paste over this release agent coating (c).

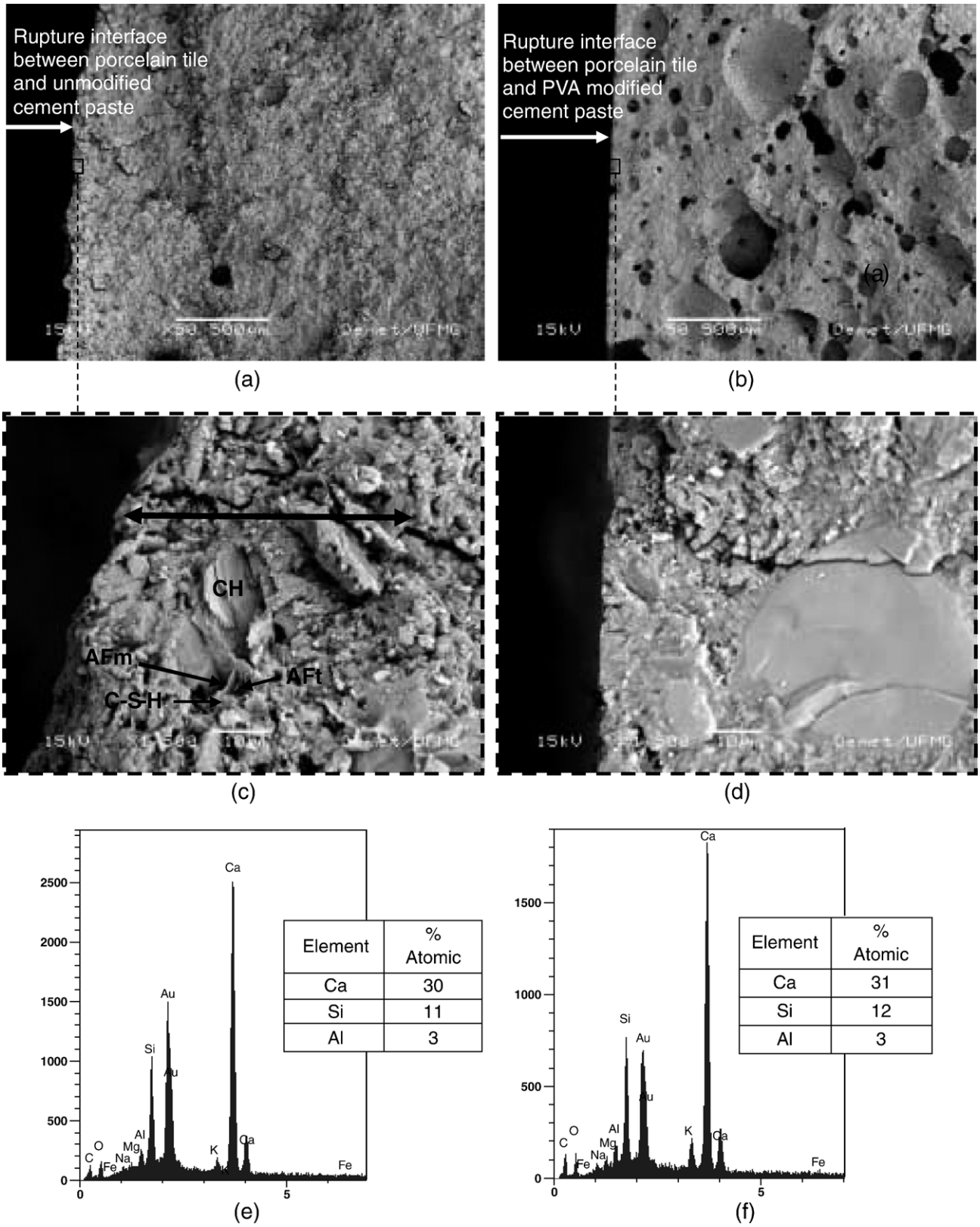

Fig. 2. Backscattered electron micrograph of the interface between porcelain tile and (a, c) unmodified cement paste (arrow indicates interfacial transition zone thickness) and (b, d) PVA modified cement paste (BSE, magnification: 50× and 1500×). EDS spectra of (e) transition zone of unmodified cement paste and (f) PVA modified cement paste near interface.

conducted with degrees of hydrolysis in the range from 80 to 100%. Also, partially hydrolyzed grades of PVOH (87.0–89.0%) are generally favored as protective colloid in EVA emulsion polymerization. The selection of PVA was driven mostly by its low molecular weight which allows the reduction of the amount of water necessary to promote paste spread in order to minimize drying shrinkage in an attempt to avoid detachment during drying (an alternative choice for other PVA would demand a higher water to cement ratio). Besides that, it is important to remember that degree of hydrolysis has a dynamic behavior under alkaline conditions [6].

Commercial porcelain ceramic tiles with water absorption less then 0.5%, according to the manufacturer, were used as substrate for cement paste application.

2.2. Methods

PVA was supplied as powder and the aqueous solution was prepared by dissolving 10.0 g of polymer powder in 100 ml of deionized water. Firstly, PVA was dispersed in water at room temperature (25±2) °C using sufficient magnetic stirring to wet out all particles. After 5 min, the temperature was increased to (75±2) °C and the magnetic stirring was reduced, avoiding foam formation, in order to allow full dissolution of PVA. Then, polymer solution was let to cool down to room temperature before use.

The cement powder was mechanically mixed for 3 min with water or PVA solution with a water/cement (w/c) ratio of 0.50 wt.%. The previously prepared PVA solution was diluted with water in order to obtain polymer to cement (p/c) ratio of 2.0 wt.%. Cement paste was left to rest for 10 min covered by a humid cloth, before the application.

A single layer cement paste with average thickness of 6 mm was applied on the back side of each porcelain ceramic tile, followed by the application of a 0.05 kgf/cm^2 load for 45 s to promote cement paste spreading and penetration into surface roughness. The porcelain tiles with cement paste were covered with a plastic film and stored in laboratory for 14 days when the plastic was removed.

SEM images were taken from fractured surfaces of porcelain tile and paste/tile system after 56 days with a JSM 6360LV, Jeol/Noran, microscope coupled to Energy Dispersive Spectrometer (EDS) for semi-quantitative chemical analysis. Before examination, samples were coated with a thin gold film by sputtering using low deposition rate, cooling of substrate and maximum distance between target and sample in order to avoid sample damage. Images of secondary electrons (SE) and backscattered electrons (BSE) were obtained using an accelerating voltage of 15 kV.

In order to evaluate the degree of hydration, XRD patterns and FTIR spectra were obtained. XRD assays were conducted in PW1710, Philips, that uses CuKα radiation with $\lambda = 1.5406$ Å, in the range of 2Θ from 5° to 60°. FTIR spectroscopy with diffuse-reflectance accessory (Perkin-Elmer, Paragon 1000) was used. Samples were placed in a sampling cup and 32 scans were acquired at 2 cm^{-1} resolution with the subtraction of KBr background (4000 to 400 cm^{-1}). Before XRD and FTIR analyses, samples were crushed and sieved (# 200 mesh).

3. Results and discussion

3.1. Effects of PVA on cement paste/porcelain tiles interface

In both samples of cement paste/porcelain tile, with and without PVA, paste has debonded from ceramic tile due to

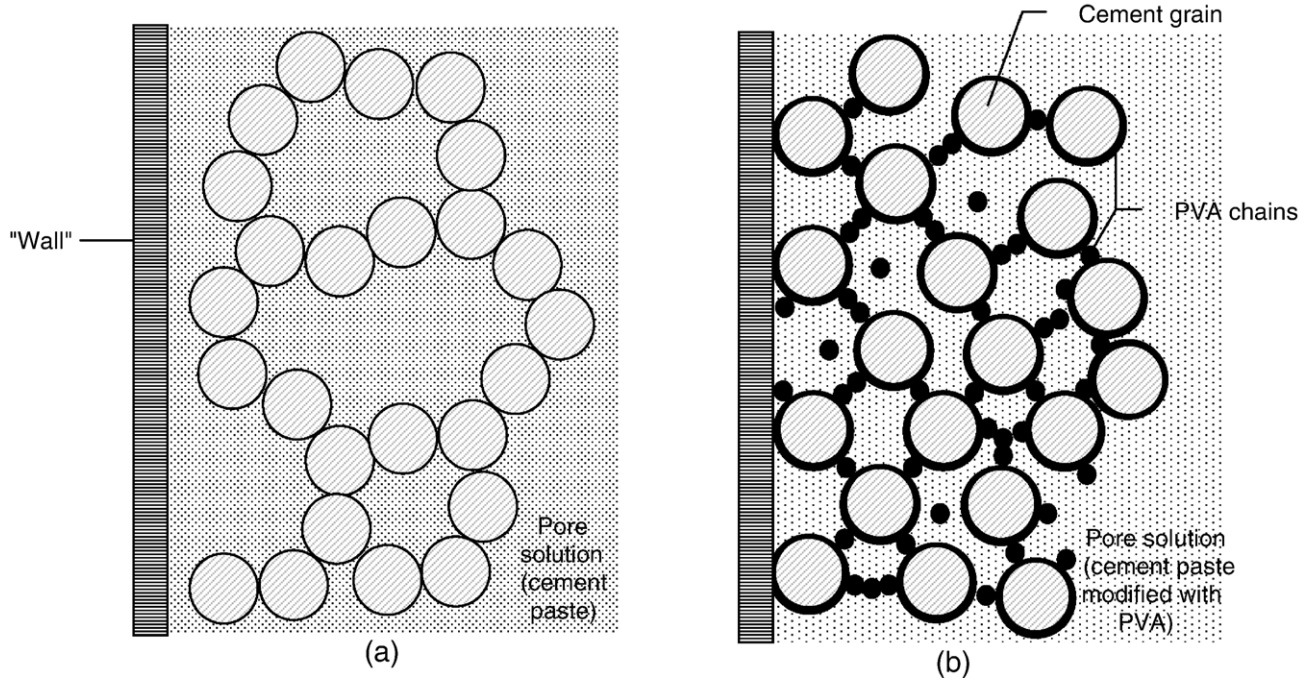

Fig. 3. Schematic drawings showing “wall effect” and bleeding in cement pastes (a) without PVA and (b) modified with PVA (not in scale).

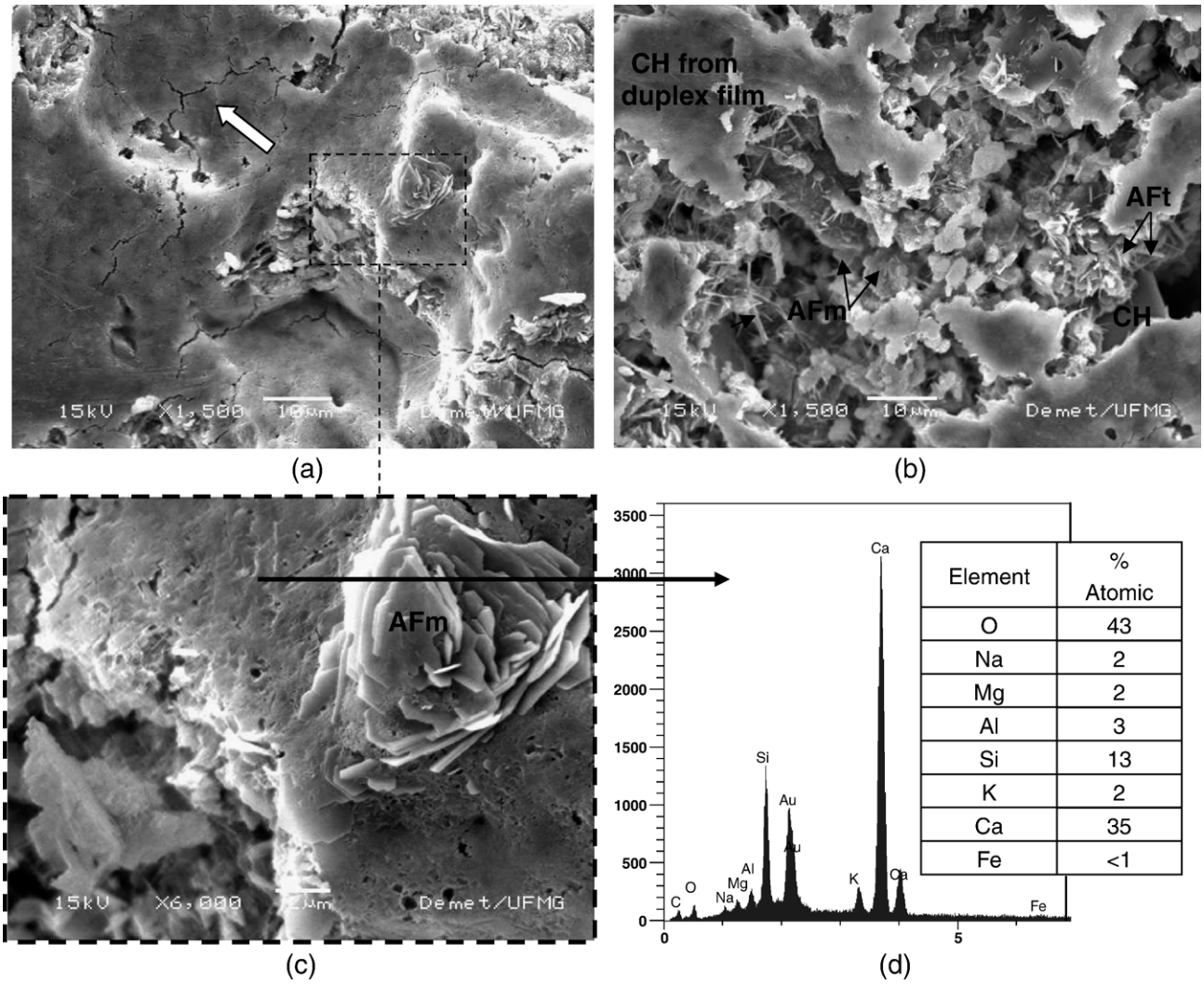

Element	% Atomic
O	43
Na	2
Mg	2
Al	3
Si	13
K	2
Ca	35
Fe	<1

Fig. 4. SEM micrographs of debonded unmodified cement paste surface. (a) Large smooth areas corresponding to microscopically adhesive rupture of paste from porcelain tile (SE, magnification: 1500×). (b) Areas of mostly cohesive rupture of unmodified cement pastes (SE, magnification: 1500×). (c) Detail of adhesive rupture layer (from paste side) with EDS spectrum (d) of duplex layer (SE, magnification: 6000×).

shrinkage. In the case of cement paste without PVA, paste split away from the tile after 14 days during the curing period. For cement paste modified with polymer, debonding has occurred during sample manipulation after 56 days. Debonding by shrinkage was observed by others authors during drying [4,18]. However, macroscopically, the specimen failure mode was found to change with the addition of PVA. The mode changed from mostly interfacial failure without PVA (Fig. 1a) to a mixed-mode interfacial-cohesive failure of the paste with addition of PVA (Fig. 1b).

The presence of engobe on the back side of the tile can also be seen in these images of Fig. 1. During ceramic firing, engobe is a coating of a release agent that prevents fusion of the tile to kiln surface. Considering ceramic tiles with high water absorption properties, the presence and extension of this coating reduces the adhesive bond between tile and cement based materials because it acts as barrier reducing the interfacial contact, especially if it is loosely bonded to ceramic tile back side [19]. However, in the case of porcelain tiles with very low degree of water absorption, it could act as a point of mechanical anchoring of cement paste to tile associated with its high porosity. Therefore, the efficiency of this linkage is dependent on how tight this engobe is on the backside.

SEM images (not shown) from the back surface of the porcelain tile have revealed the porosity of engobe in contrast with the almost absence of pores in porcelain tiles resultant from its composition and processing. It is important to note that for paste modified with PVA, cohesive rupture of cement paste has not coincided with these engobe areas, while for the unmodified paste some of the few points of cohesive failure were in agreement with engobe presence (Fig. 1c).

Micrographs of the interface formed by the porcelain tile and cement pastes are shown in Fig. 2 for unmodified and PVA modified pastes. First of all, it was noteworthy the difference in porosity of these two pastes. This was expected because PVA is a surface active agent that stabilizes the air voids that are formed in cement based materials by whipping of air into the mix from surface during mechanical mixing [14,20]. In second place, the

cement paste with poly(vinyl alcohol) has presented an interface well defined, almost parallel to the porcelain tile surface, even at microscopic level. Also, the transition zones in the hardened paste adjacent to flat tile surfaces were quite different. In samples without PVA, one can easily observe a porous layer extending away from the interface by 25 to 50 μm to the paste bulk (Fig. 2c). For the paste with PVA, almost no porosity can be seen and the transition zone either was not present or it was limited to 10 μm (Fig. 2d). Similar results of reduction of interfacial transition zone width and porosity were previously reported by Kim et al. when studying ITZ between plain and PVA modified pastes and aggregates [2,4].

Concerned with composition of these layers, EDS spectra over general area of the samples inspected at a magnification of 1500× were obtained and are shown in Fig. 2e and Fig. 2f. For unmodified pastes, the transition zone was composed of calcium hydroxide (CH) platelets some of them with some degree of preferential orientation with respect to the tile surface (parallel). The presence of hydrated calcium silicates (C–S–H) type II, CH, ettringite needles (AFt phase — Al_2O_3–Fe_2O_3-tri) and monosulfoaluminate plates (AFm phase — Al_2O_3–Fe_2O_3-mono) was also observed. The calcium/silicon (Ca/Si) ratio was found to be 2.7 at% (atomic percent). This value was higher than the expected for Ca/Si in C–S–H matured pastes, ranging from 1.5 to 2.0, associated with the presence of CH [21]. Considering the image acquired for mature modified paste, due to its high densification, it was difficult to identify the isolated hydrated cement phases on fractured surfaces. No significant difference on the Ca/Si ratio was observed for modified and unmodified paste (Ca/Si = 2.6). Besides that, the presence of cement grains at a 50 μm distance from the interface with higher dimensions than usually expected in plain cement pastes [22] was remarkable and the density of the paste in this area appeared almost the same as that in the bulk paste for which we have calculated a similar Ca/Si ratio equal to 2.8 based on EDS results (not shown).

This phenomenon can be explained by the same reasons that cause the formation of interfacial transition zone (ITZ) between aggregate particles and cement paste: wall effect and bleeding [4,23–26]. The wall effect arises from the flocculation of cement particles [4,23] to form loosely organized structure which leads to a depletion of anhydrous cement in the interfacial zone, approaching to zero at aggregate surface [25]. Packing of large flocs at aggregate surface may leave large solution-filled spaces between the flocs and the aggregate surface. Bleeding arises from the settling of cement particles, either individually or as flocculated units, leaving a layer of water over cement based materials surface [20] and beneath large aggregate particles [18]. Mixing and vibration may also accelerate the bleeding around aggregates [4,26]. Then, the effect of the anhydrous cement packing and bleeding at aggregates surfaces means that there is a higher effective water to cement ratio at interfacial zone resulting in the increased porosity, larger crystals of hydrated products and lower bond strength [25–28]. The addition of PVA to cement based materials alters the state of flocculation/coagulation of cement [4]. Poly(vinyl alcohol) chains adsorbed onto cement surfaces and/or in solution substitute interactions cement–cement by interactions cement–polymer–cement or cement–polymer–water–polymer–cement resulting in well-dispersed cement particles, even though the suspension remain flocculated due to PVA interactions [29]. Also, bleeding was found to be reduced with the PVA modification of mortars [2]. So, PVA addition raises the solid–liquid ratio at the interface improving the interfacial bond by pore refinement and grain refinement processes (Fig. 3).

Studies have reported that the size of ITZ, on average, is between 35 and 50 μm, although some authors have already estimated the distance between aggregate surface and bulk characteristic microstructure to be about 100 μm [21,30]. The development of nanostructure and microstructure of ITZ has been subjected of extensive research and it was reviewed by Diamond [31]. Summarizing from that review, with various and some contradictory results, the principal feature of the interfacial microstructure is a duplex film. The duplex film occurs immediately adjacent to the aggregate surface. The side of the film in contact with the aggregate is a layer of CH (0.5 μm thick) followed by a thin layer of C–S–H gel in the form of short fibers that extended into the cement paste [23]. In microstructure work since Diamond's review, descriptions of the overall features of interfacial microstructure have been similar in most but not all aspects, especially by the fact that some authors have not observed a duplex film but a single film of C–S–H [18,30,32,33] or CH [24,27]. It is interesting to note that several works have used the specimen configuration in which cement paste is cast onto a large flat piece of aggregate [4,18]. This kind of specimen, very similar to ceramic tile condition, allows the concentration of and orientation of phases in the interfacial region. In such studies it has been found that CH has a preferred orientation in the interfacial region and that there is a trend to form more ettringite near to aggregate surface [18].

Fig. 4 shows the failure interface (from the paste side) between the unmodified paste and the porcelain tile. Two distinct regions can be observed on the surface of the cement paste. A large area of the surface was smooth and had separated cleanly from the tile (Fig. 4a). The other area has been mostly cohesive failure in the paste (Fig. 4b) with the surface layer remaining adhered to the ceramic tile.

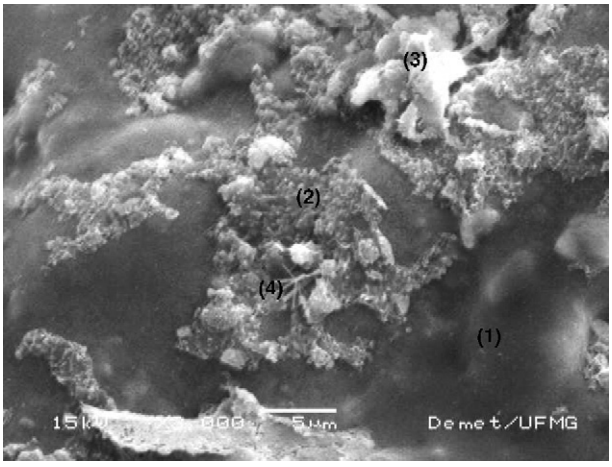

Fig. 5. SEM image of unmodified paste/porcelain tile interface (tile side) (SE, magnification: 3000×). (1) Porcelain tile surface; (2) duplex film; (3) hydration products; (4) ettringite needles.

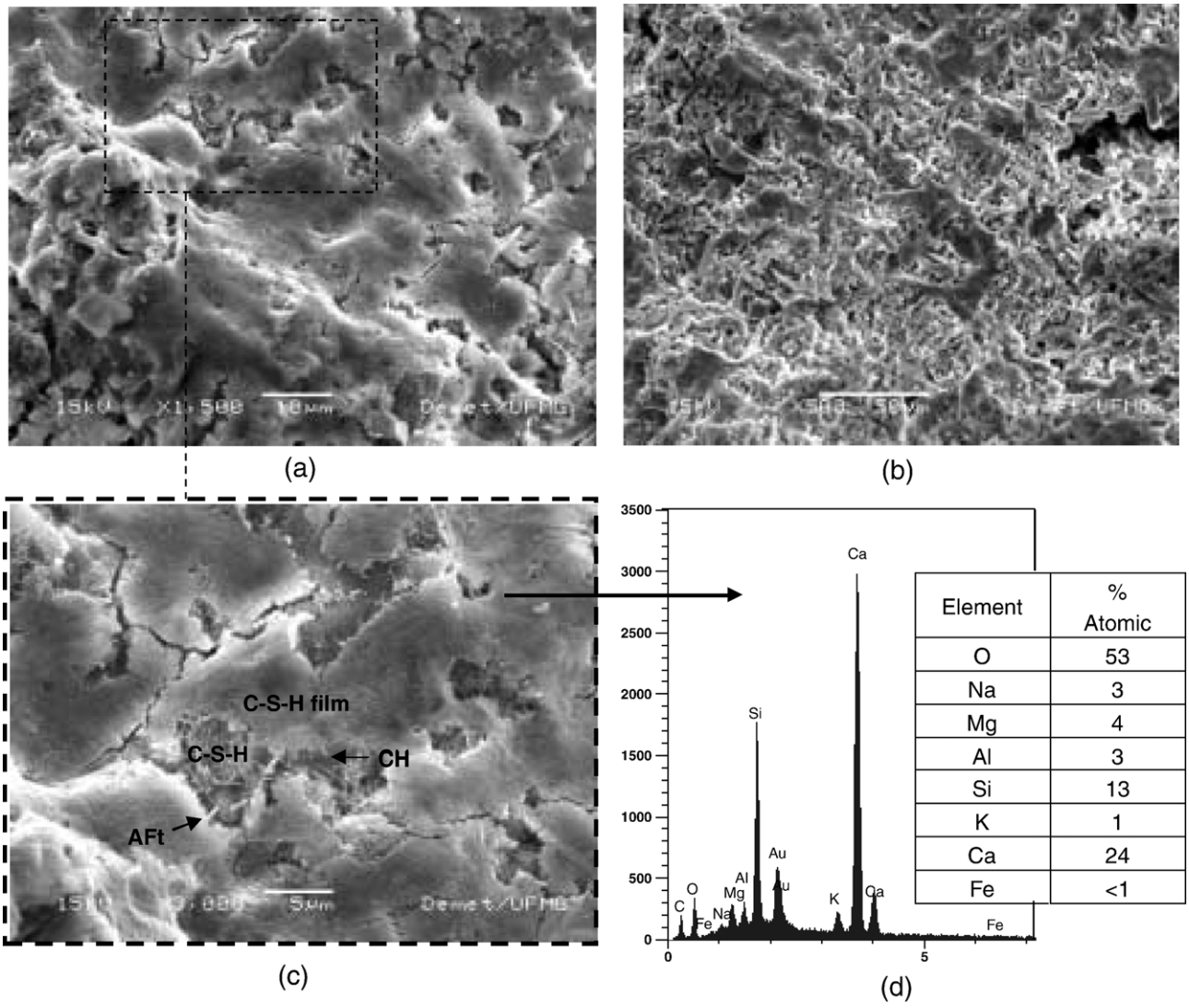

Element	% Atomic
O	53
Na	3
Mg	4
Al	3
Si	13
K	1
Ca	24
Fe	<1

Fig. 6. Adhesive failure surface from modified paste surface side (a, b) (SE, magnification: 1500× and 500×, respectively). (c) Detail of adhesive rupture layer of smooth areas of adhesive surface of rupture (paste side) with EDS spectrum (d) (SE, magnification: 3000×).

A detail of the area of adhesive rupture from unmodified paste side can be observed in Fig. 4c. The material in contact with the porcelain tile surface appeared layered with minimal crystallinity, with less than 1 μm thick. This layer has the appearance of duplex film as reported by several works [34–36]. Based on EDS spectra in this area (Fig. 4d), the Ca/Si ratio was about 2.7 which is characteristic of a composition involving CH and C–S–H. SEM investigation also highlighted cracking of interfacial zone (arrow in Fig. 4a). It is believed that the disrupted damaged structure was caused by drying shrinkage and volume changes during hydration [18,26]. Other possibility was cracking during vacuum drying of specimens prior to gold coating for SEM examination [35]. In Fig. 4c, one also can also identify the presence of cluster of AFm plates. Some authors reported the presence of some ettringite at aggregate surface and its conversion to monosulfate during cement hydration [37].

The area of cohesive rupture in paste revealed the interfacial zone of high porosity enriched with ettringite needles, monosulfate plates, large CH crystals, some of them with preferential orientation (*c*-axes normal to the interface), and C–S–H type II (Fig. 4b). Concentration of ettringite has been observed in the interfacial region because the small cement particles that occupy this area tend to have more interstitial material (aluminate and ferrite phases) exposed on their surfaces [18]. Also the high water/cement ratio favors precipitation of AFt phases in this area [38]. Monosulfate is formed from ettringite reaction with aluminate (C_3A) phases during hydration [21]. Large CH crystals are present because there is more space for the crystal growth in this interfacial area [18,23,38]. The orientation effect of CH can be thermodynamically explained by the plane (001) of the $Ca(OH)_2$ crystals that must be parallel to the aggregate surface in order to maintain the stable state of minimum energy. However, some factors such as water/cement ratio, curing age, kind of aggregate, roughness of the aggregate surface, admixtures, and so on, influence the orientation of CH [39]. Finally, the infilling with this region with a C–S–H gel is related to the rapid hydration of the relatively small cement particles which tend to collect there [18].

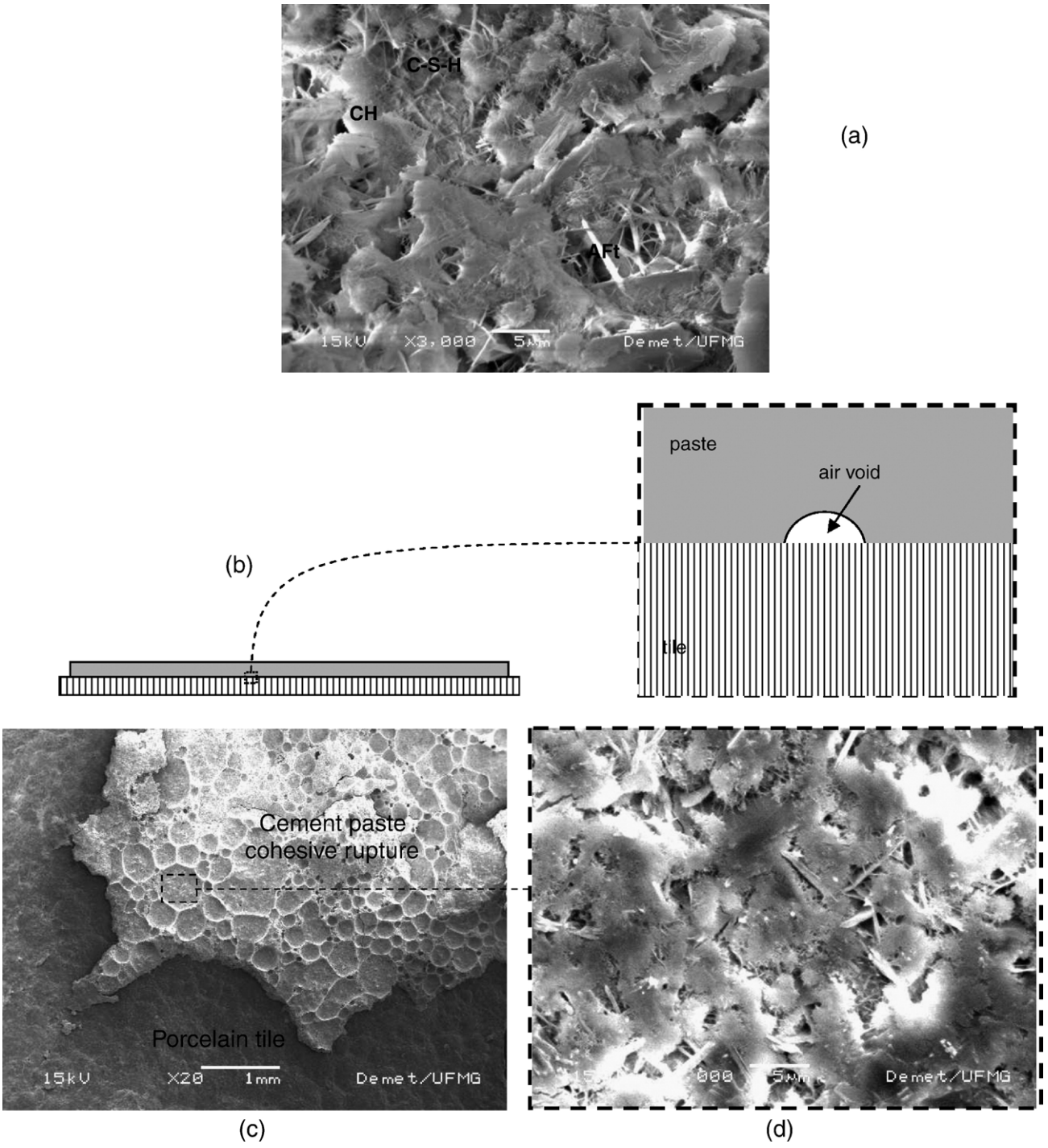

Fig. 7. (a) SEM image of irregular surface at adhesive failure interface (SE, magnification: 3000×). (b) Air entrapment at paste/tile interface (not in scale). (c and d) SEM image of the mixed mechanism of failure verified for PVA modified cement pastes with a detail of cohesive rupture surface at modified cement paste (tile side) (SE, magnification: 20× and 3000×).

The detailed surface failure of porcelain tile is shown in Fig. 5. It was possible to observe some clean areas, where duplex films were peeled off from the tile, revealing porcelain surface (1), a dense hydrated layer associated with the duplex film (2), plus some additional coarser material attached to the duplex film (3), including some ettringite needles (4).

As previously shown in Fig. 1b the mechanism of failure was different for sample of PVA modified cement paste when compared to plain cement paste. In this case, even macroscopically, a mixed failure mode was observed. Separation directly at the porcelain surface has occurred but failure was also verified further away from the interface and significant amounts of hydrated material remained adhered to the tile surface.

Failure adhesive interface (from the paste side) between polymer modified paste and the porcelain tile is shown in Fig. 6 where one can observe a smooth area Fig. 6a and an irregular surface Fig. 6b.

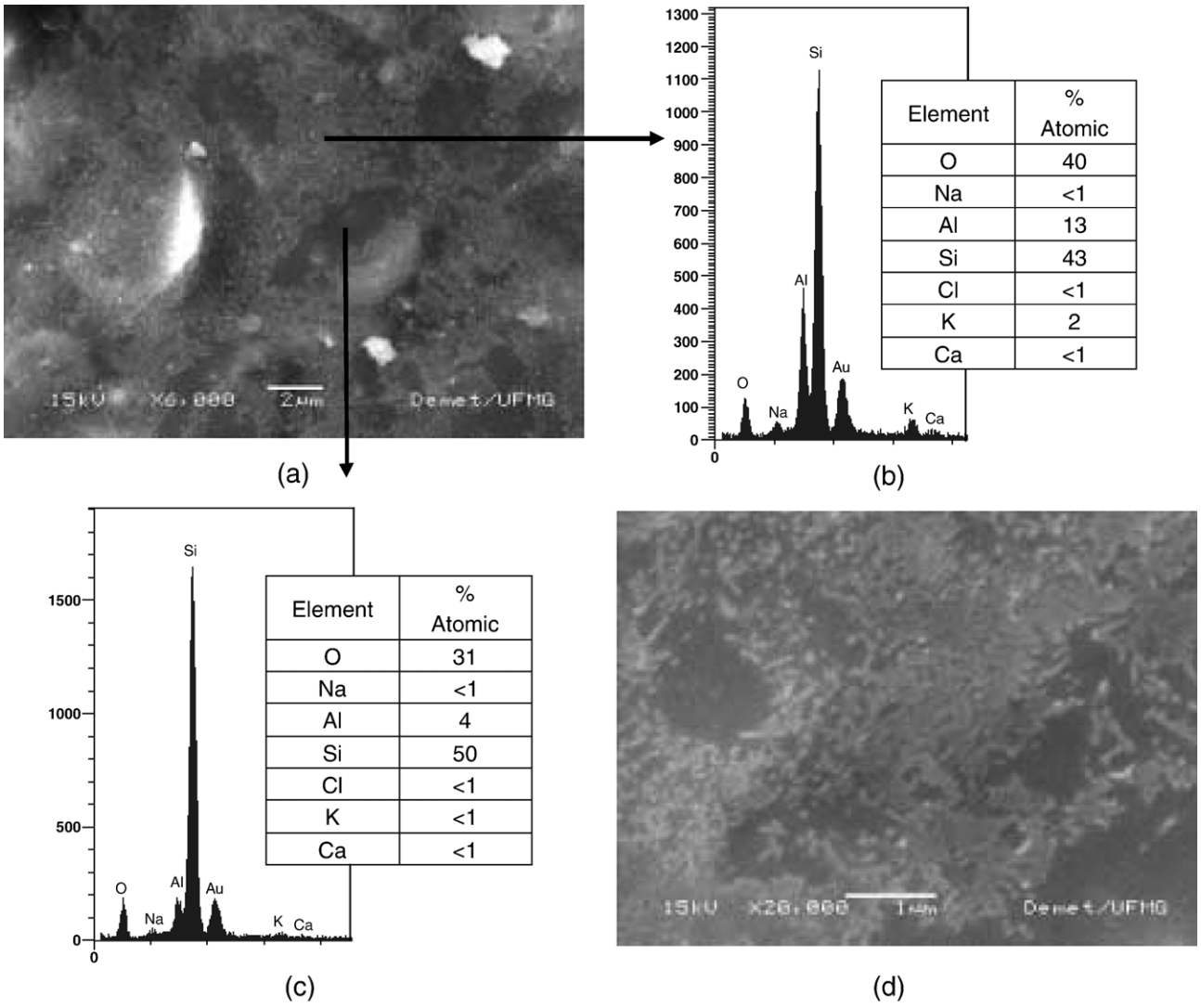

Fig. 8. (a) Porcelain tile surface in adhesive rupture area (from tile side) with EDS spectra of different features: (b) area with and (c) without submicrometric material (SE, magnification: 6000×). (d) SEM micrograph of submicrometric material adhered onto glass surface of porcelain tile (SE, magnification: 20,000×).

The smooth region is detailed in Fig. 6c. This smooth area has presented the typical morphology of outer C–S–H gel with less evidence of fibrils orientation from tile surface. EDS of this layer (Fig. 6d) showed a Ca/Si ratio of about 1.8, a value that lies in the typical range of C–S–H phases. The C–S–H film was followed by a denser region, when compared with the transition zone of unmodified paste shown in Fig. 4b, rich in C–S–H phase and with some ettringite (AFt) and portlandite (CH). The images also indicated the presence of cracks on this surface layer.

A possible explanation for the differences between the hydrated films developed at interface paste/porcelain tile, for unmodified and modified pastes, may be in the changes introduced by PVA addition. As already stated PVA modification reduces water/cement ratio at interfaces, by increasing the amount of cement grains near interface and avoiding bleeding. Also, the introduction of polymer chains increases the viscosity of the solution reducing ions mobility and dissolution [1,3,4,40,41]. According to Zhang et al. [32] these aspects may favor the formation of initial coating of C–S–H onto aggregate surfaces because many data of pore solution analysis suggest that supersaturation with respect to C–S–H occurs well before that with respect to CH and so C–S–H might be expected to nucleate first. The absence of bleeding areas of high water/cement ratio and the reduced mobility of ions help in avoiding calcium ions to reach aggregate surface which may result in a supersaturation/precipitation of CH phase at interface.

The area of irregular shape on the adhesive failure surface of modified paste (Fig. 6b) is shown in detail in Fig. 7a. In this region one can identify acicular C–S–H, ettringite and CH. It is believed that this morphology was related to regions where air bubbles were entrapped at interface when mortar was applied onto ceramic surface [42] especially due to the surfactant effect of poly(vinyl alcohol) that stabilizes bubbles (Fig. 7b). It is interesting to note that the surface cohesive rupture in modified cement paste, which has occurred revealing bubbles surfaces (Fig. 7c), has presented similar morphology (Fig. 7d) to the observed at the irregular areas.

Fig. 8 shows the porcelain tile surface which had been in contact with the modified cement paste (adhesive rupture). At magnifications of less than 3000× (not shown) the surface has presented the smooth texture characteristic of the silicate glassy

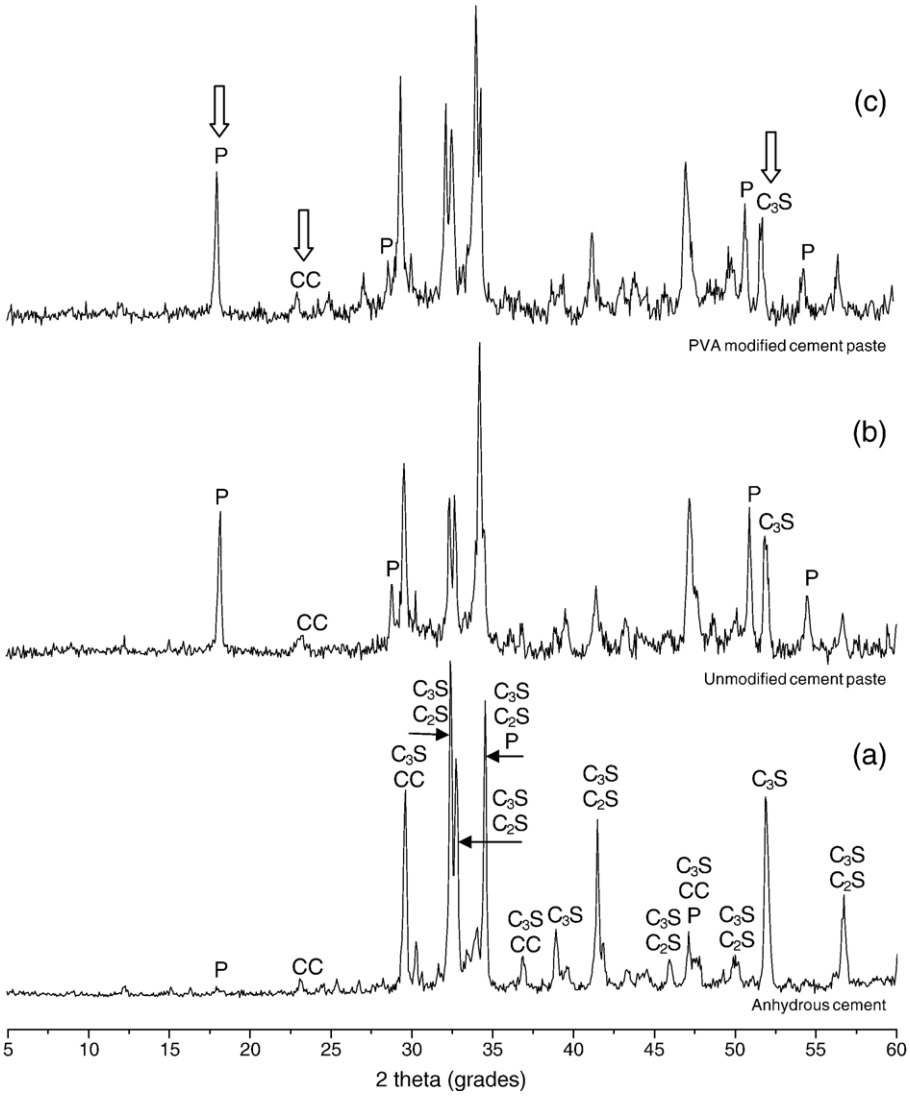

Fig. 9. XDR patterns of (a) anhydrous cement, (b) unmodified cement paste, and (c) cement paste modified with 2 wt.% of PVA (56 days of age).

phase [43] that constitutes porcelain ceramic tiles, without areas of visible hydration products detectable. However, at higher magnifications (Fig. 8a and d), a submicrometric material can be seen adhered to porcelain surface with missing areas in high quartz (SiO_2) content composition regions (probably quartz grains near tile surface).

It is well established that quartz particles are among the less reactive aggregates with, generally, no indication of reactions at their surfaces when in contact with cement based materials [32,44]. By the other side, silica glass is a strongly reactive aggregate [32]. Silica and silicate glasses based on $(SiO_4)^{4-}$ tetrahedral have a random three-dimensional network without any periodicity or symmetry. Nevertheless, the continuous Si–O–Si structure of SiO_2 is sometimes interrupted by defects such as silanol groups (Si–OH), which are mostly present at surfaces [45]. Glasses in contact with water will be chemically attacked in two very general stages. The first is a selective leaching of mobile ions from bulk of solid through the surface and interface (diffusion). The second is a process of water dissolution of silica network with hydrolysis of Si–O–Si bonds. Hydration of the silica after hydrolysis will form new silanol groups as a consequence of the reaction of the silicon–oxygen bonds with water. The presence of hydroxyls (high pH values similar to cement pore solution) leads to faster dissolution of silica favoring the formation of new Si–OH and SiO^- defects [45,46]. Based on that, some explanations for the submicrometric material may be addressed. First, once dissolution of silica glass is considerably reduced in basic solutions containing calcium ions, some authors believe that a layer of calcium silicates is formed at silica surface working as a protective film [45]. Zhang et al. [32], through transmission electron microscopy, have detected the coating of silica glass aggregates with a layer of smooth gel material about 200 nm in depth. As a consequence, it was proposed that such deposits in the present study are likely to be caused by interactions between C–S–H fibrils (interface of modified paste/porcelain tile) and tile surface. For poly(vinyl alcohol)-free paste samples, as it was identified a duplex film at interface, these structures were not expected to be found. Besides that, rooted in literature [16,47], it may be considered the formation of a hybrid polymer–ceramic interface by hydrogen bonds between hydroxyl groups of PVA

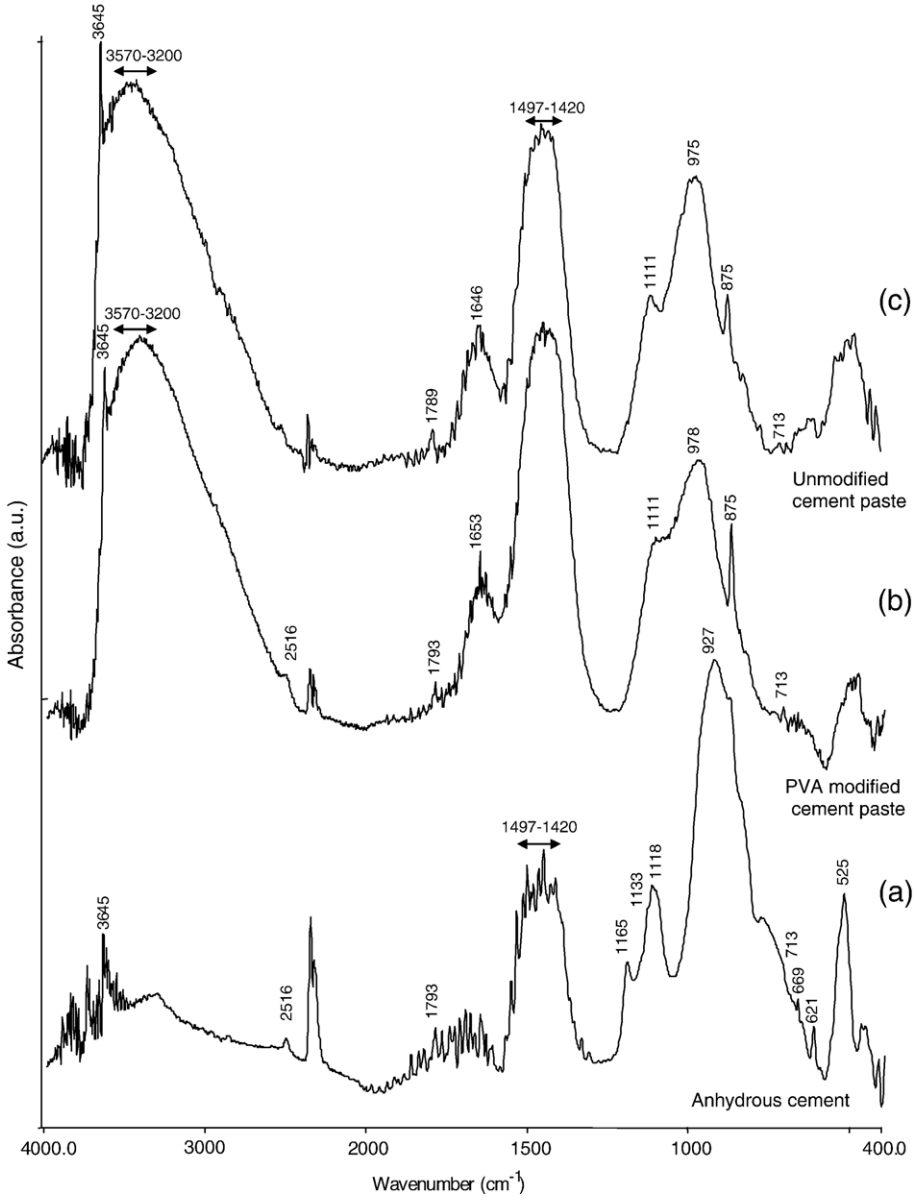

Fig. 10. FTIR spectra of (a) anhydrous cement, (b) unmodified cement paste, and (c) cement paste modified with 2 wt.% of PVA (56 days of age).

and silanol from glass surface or between C–O^- from deprotonated hydroxyl of PVA and $(SiO_2)^-$ defects on glass surface. Also, considering the development of a C–S–H layer at the interface, one may also propose that the usual van der Waals interactions between polymers and cement matrix may have been substituted by much stronger forces associated with hydrogen bonds involving PVA and non-bound water from C–S–H gel (interlayer and adsorbed water molecules) [21].

3.2. Effects of PVA on degree of hydration

In order to investigate the influence of the polymer on the cement hydration in the modified paste, XRD patterns of the pastes with and without PVA were obtained and are displayed in Fig. 9 with XRD curve for anhydrous cement (Fig. 9a). Upon hydration the Portland cement main phases, C_3S (tricalcium silicate — alite) and C_2S (dicalcium silicate — belite), produce mainly portlandite $Ca(OH)_2$ and amorphous calcium–silica–hydrate (C–S–H). The cement used in this study already has some carbonate addition. Therefore, additional $CaCO_3$ phase was detected as a result of secondary reactions of $Ca(OH)_2$ and C–S–H with atmospheric CO_2 [8,21,48,49].

The degree of hydration could be estimated by comparing the peaks corresponding to $Ca(OH)_2$ and C_3S ($3CaO \cdot SiO_2$ — tricalcium silicate). With more hydration, the relative surface area of the peak associated with portlandite will increase and that of C_3S will decrease [8]. It is also important the evaluation of carbonation, that is the increase in $CaCO_3$ content. Among the several peaks of the interest phases in these patterns, calcium hydroxide peak at interplanar distance $d = 4.92$ Å ($2\Theta \approx 18°$), tricalcium silicate peak at $d = 1.76$ Å ($2\Theta \approx 52°$), and calcium carbonate peak at $d = 3.84$ Å ($2\Theta \approx 23°$) were chosen because each one of them is representative of only a single phase, without peak overlapping.

In both samples of cement pastes the intensity of the peaks related to C_2S and C_3S diminished while strong peaks associated with the formation of portlandite appeared. Statistical analysis from XRD patterns revealed that there is no significant difference between the degrees of hydration of both pastes under evaluation. Calcite peak slightly increased in both pastes, mostly in modified paste, when compared with anhydrous cement. Based on literature, PVA addition retards setting time of cement paste [4], but it has a weak influence on the silicate condensation as detected by ^{29}Si NMR [50].

FTIR spectroscopy allows the evaluation of degree of polymerization of silicate units in cement based materials and the influence of organic admixtures in $(SiO_4)^{4-}$ group condensation [51,52]. FTIR spectra for the samples under evaluation are shown in Fig. 10.

The spectrum of anhydrous cement clearly revealed the major peaks of silicates due to Si–O asymmetric stretching vibration (ν_3=927 cm^{-1}) and Si–O out of plane bending vibration (ν_4=525 cm^{-1}). The bands associated with gypsum and anhydrite that appeared in the range 1165 to 1096 cm^{-1} are due S–O stretching vibration (ν_3) of $(SO_4)^{2-}$, and the peak at 669 cm^{-1} is due bending (ν_4) vibrations of $(SO_4)^{2-}$. Band at 621 cm^{-1} is also related to anhydrite. Carbonates bands (2516 cm^{-1}, 1793 cm^{-1}, 1497–1420 cm^{-1}, 875 cm^{-1}, and 713 cm^{-1}) in dry cement are mostly associated with cement mineral admixture. The band at 3545 cm^{-1} comes from traces amount of water present [51,53,54].

The spectral data changes upon cement pastes hydration with and without poly(vinyl alcohol) have indicated the formation of portlandite by the increase on the peak at 3645 cm^{-1}, due to the OH band from $Ca(OH)_2$. The broad band in the range from 3570 to 3200 cm^{-1} is related to symmetric and asymmetric (ν_1 and ν_3) stretching vibrations of OH adsorbed water molecules. Also, one can observe the water bending vibrational (δ) peak around 1650 cm^{-1}. Considering sulfate phases upon hydration, the bands shifted toward a lower wavenumber caused by ettringite formation (1111 cm^{-1}). The raising in carbonates bands in both modified and unmodified samples arisen from the reactions of hydrated phases with atmospheric CO_2 as already stated. It is important to point out that FTIR was used as a qualitative technique in order to evaluate hydration.

The peaks associated with silicates also underwent changes during hydration, the most evident being the shifting of the Si–O asymmetric stretching vibration (ν_3=927 cm^{-1}) to higher wavenumber. This shifting indicates polymerization of the silicate units $(SiO_4)^{4-}$ and it is considered a fingerprint evidence for degree of polymerization with the formation of C–S–H phase [51]. Based on FTIR spectra, the degree of polymerization of both samples were quite similar.

4. Conclusions

The conclusion drawn from the current studies are summarized as follows:

1. Modification of cement pastes with poly(vinyl alcohol) improved adherence between the paste and porcelain tiles. The mode of rupture changed from mostly interfacial failure without PVA to a mixed-mode interfacial-cohesive failure for the paste with polymer addition in a macroscopically evaluation.
2. PVA addition has reduced the thickness of the porous transition zone between porcelain tile and dense cement paste bulk.
3. In cement paste without PVA it was observed the formation of a duplex film (CH followed by C–S–H) in contact with the porcelain tile surface. In polymer modified cement paste a single layer of C–S–H was identified.
4. PVA addition has not affected adversely cement hydration at least at higher ages.

Acknowledgments

The authors acknowledge financial support from the CNPq (Brazilian Council of Research). Also we are grateful to Laboratory of Ceramic Materials (Prof. Wander Luiz Vasconcelos), Laboratory of Electron Microscopy (Patrícia Mara Trigueiro de Azevedo) and Laboratory of X-Ray Diffraction (Prof. Vicente Tadeu Lopes Buono e Andréia Bicalho Henriques). Poly(vinyl alcohol) and cement were kindly supplied by Celanese Chemicals and Cimento Tupi, respectively.

References

[1] Y. Ohama, Polymer-based admixtures, Cem. Concr. Res. 20 (2–3) (1998) 189–212.
[2] J. Kim, R.E. Robertson, A.E. Naaman, Structure and properties of poly (vinyl alcohol)-modified mortar and concrete, Cem. Concr. Res. 29 (3) (1999) 407–415.
[3] N.B. Singh, S. Rai, Effect of poly(vinyl alcohol) on the hydration of cement with rice husk ash, Cem. Concr. Res. 31 (2) (2001) 239–243.
[4] J. Kim, R.E. Robertson, Effects of polyvinyl alcohol on aggregate–paste bond strength and the interfacial transition zone, Adv. Cem. Based Mater. 8 (2) (1998) 66–76.
[5] R.S. Santos, F.A. Rodrigues, N. Segre, I. Joekes, Macro-defect free cements Influence of poly(vinyl alcohol), cement type, and silica fume, Cem. Concr. Res. 29 (5) (1999) 747–751.
[6] J. Rottstegge, M. Arnold, L. Herschke, G. Glasser, M. Wilhelm, H.W. Spiess, W.D. Hergeth, Solid state NMR and LVSEM studies on the hardening of latex modified tile mortar systems, Cem. Concr. Res. 35 (12) (2005) 2233–2243.
[7] A. Jenni, L. Holzer, R. Zurbriggen, M. Herwegh, Influence of polymers on microstructure and adhesive strength of cementitious tile adhesive mortars, Cem. Concr. Res. 35 (1) (2005) 35–50.
[8] W. Jingang, Z. Shuxiang, Y. Haiqin, K. Xiangzheng, W. Xikui, G. Zhongmao, Study of cement mortars modified by emulsifier-free latexes, Cem. Concr. Compos. 27 (9–10) (2005) 920–925.
[9] W.C. Wuan, Tiling failures — a chronic problem re-visited, Proc. VIII World Congress on Ceramic Tile Quality, Castellon, Spain, 2004, pp. PGII49–PGII56.
[10] C. Diaz, Ceramic tile pathologies, Proc. VIII World Congress on Ceramic Tile Quality, Castellon, Spain, 2004, pp. PD3–PD9.
[11] C. Cass, Achieving 100% adhesive coverage, Proc. VIII World Congress on Ceramic Tile Quality, Castellon, Spain, 2004, pp. PGII99–PGII107.
[12] A.A.P. Mansur, O.L. Nascimento, H.S. Mansur, Data collection of five years of exterior facade pathologies in Brazil, Proc. IX World Congress on Ceramic Tile Quality, Castellon, Spain, 2006, pp. PBB107–PBBI20.
[13] M. Abreu, V. Leitão, J.C. Lucas, Modeling the behavior of ceramic tile covering, Proc. VIII World Congress on Ceramic Tile Quality, Castellon, Spain, 2004, pp. PGII3–PGII17.
[14] J. Kim, R.E. Robertson, Prevention of air void formation in polymer-modified cement mortar by pre-wetting, Cem. Concr. Res. 27 (2) (1997) 171–176.

[15] F.A. Rodrigues, I. Joekes, Macro-defect free cements: a new approach, Cem. Concr. Res. 28 (6) (1998) 877–885.
[16] R.N. Edmonds, A.J. Majumar, The hydration of an aluminous cement with added polyvinyl alcohol-acetate, J. Mater. Sci. 24 (1989) 3813–3818.
[17] K.M. Atkins, R.N. Edmonds, A.J. Majumdar, The hydration of Portland and aluminous cements with added polymer dispersions, J. Mater. Sci. 26 (1991) 2372–2378.
[18] K.L. Scrivener, E.M. Gartner, Microstructural gradients in cement paste around aggregate particles, in: S. Mindess, S.P. Shah (Eds.), Bonding in Cementitious Composites, Materials Research Society, Pittsburgh, 1988, pp. 77–85.
[19] R.P. Goldberg, Directed Adhered Ceramic Tile, Stone and Thin Brick Facades, Latricrete International, Bethany, 1998.
[20] T.C. Powers, The Properties of Fresh Concrete, John Wiley & Sons, New York, 1968.
[21] H.F.W. Taylor, Cement Chemistry, Thomas Telford, 1997.
[22] K.L. Scrivener, Backscattered electrons imaging of cementitious microstructures: understanding and quantification, Cem. Concr. Compos. 26 (8) (2004) 935–945.
[23] L. Struble, Microstructure and fracture at the cement paste–aggregate interface, in: S. Mindess, S.P. Shah (Eds.), Bonding in Cementitious Composites, Materials Research Society, Pittsburgh, 1988, pp. 11–20.
[24] A. Bentur, A. Goldman, M.D. Cohen, The contribution of the transition zone to the strength of high quality silica fume concretes, in: S. Mindess, S.P. Shah (Eds.), Bonding in Cementitious Composites, Materials Research Society, Pittsburgh, 1988, pp. 97–103.
[25] K.L. Crivener, K.M. Nemati, The percolation of pore space in the cement paste/aggregate interfacial zone of concrete, Cem. Concr. Res. 20 (1) (1996) 35–40.
[26] W. Xueqan, L. Dongxu, W. Xiun, T. Minshu, Modification of the interfacial zone between aggregate and cement paste, in: S. Mindess, S.P. Shah (Eds.), Bonding in Cementitious Composites, Materials Research Society, Pittsburgh, 1988, pp. 35–40.
[27] P.K. Metha, P.J.M. Monteiro, Effect of aggregate, cement, and mineral admixtures on the microstructure of the transition zone, in: S. Mindess, S.P. Shah (Eds.), Bonding in Cementitious Composites, Materials Research Society, Pittsburgh, 1988, pp. 65–75.
[28] S. Mindess, Bonding in cementitious composites: how important is it? in: S. Mindess, S.P. Shah (Eds.), Bonding in Cementitious Composites, Materials Research Society, Pittsburgh, 1988, pp. 3–10.
[29] A.A.P. Mansur, H.S. Mansur, The effect of PVA admixture on cement suspensions sedimentation behavior. Not submitted.
[30] D. Zampini, S.P. Shah, H.M. Jennings, Early age microstructure of the paste–aggregate interface and its evolution, J. Mater. Res. 13 (7) (1998) 1888–1898.
[31] S. Diamond, The microstructure of cement paste in concrete, Proc. 8th International Congress on the Chemistry of Cement, vol. I, Rio de Janeiro, Brazil, 1986, pp. 122–147.
[32] X. Zhang, G.W. Groves, S.A. Rodger, The microstructure of cement aggregate interfaces, in: S. Mindess, S.P. Shah (Eds.), Bonding in Cementitious Composites, Materials Research Society, Pittsburgh, 1988, pp. 89–95.
[33] O.A. Onabolu, P.L. Pratt, The effect of blast furnace slag on the microstructure of the cement paste/steel interface, in: S. Mindess, S.P. Shah (Eds.), Bonding in Cementitious Composites, Materials Research Society, Pittsburgh, 1988, pp. 255–261.
[34] I. Odler, A. Zurz, Structure and bond strength of cement–aggregate interfaces, in: S. Mindess, S.P. Shah (Eds.), Bonding in Cementitious Composites, Materials Research Society, Pittsburgh, 1988, pp. 21–27.
[35] D.G. Montgomery, A. Samarin, Adhesion between concrete and treated or untreated flat metal surfaces, in: S. Mindess, S.P. Shah (Eds.), Bonding in Cementitious Composites, Materials Research Society, Pittsburgh, 1988, pp. 263–270.
[36] T. Sugama, The effect of $Ca(OH)_2$-treated ceramic microspheres on the mechanical properties of high-temperature lightweight cement composites, in: S. Mindess, S.P. Shah (Eds.), Bonding in Cementitious Composites, Materials Research Society, Pittsburgh, 1988, pp. 301–306.
[37] R. Gallus, D. Paul, Rontgenanalyse des zementsteins im bereich der zuschlage, Dtsch Ausschuss Stahlbeton 283 (1977) 40–55.
[38] S.L. Sarkar, Y. Diatta, P.C. Aitcin, Microstructural study of aggregate/hydrated paste interface in very high strength river gravel concretes, in: S. Mindess, S.P. Shah (Eds.), Bonding in Cementitious Composites, Materials Research Society, Pittsburgh, 1988, pp. 111–116.
[39] W. Jia, Mechanism of orientation of $Ca(OH)_2$ crystals in interface layer between paste and aggregate in systems containing silica fume, in: S. Mindess, S.P. Shah (Eds.), Bonding in Cementitious Composites, Materials Research Society, Pittsburgh, 1988, pp. 127–132.
[40] Z. Su, J.M. Bijen, J.A. Larbi, Influence of polymer modification on the hydration of Portland cement, Cem. Concr. Res. 21 (2–3) (1991) 242–250.
[41] J.F. Young, A review of the mechanisms of set-retardation in Portland cement pastes containing organic admixtures, Cem. Concr. Res. 2 (4) (1972) 415–433.
[42] A. Jenni, M. Herwegh, R. Zurbriggen, T. Aberle, L. Holzer, Quantitative microstructure analysis of polymer-modified mortars, J. Microsc. 212 (2003) 186–196.
[43] E. Sanchez, M.J. Orts, J. Garcia-Ten, V. Cantavella, Efeito da composição das matérias-primas empregadas na fabricação de grês porcelanato sobre as fases formadas durante a queima e as propriedades do produto final, Cerâm. Ind. 6 (5) (2001) 15–22.
[44] W. Tasong, J.C. Cripps, C.J. Lynsdale, Aggregate–cement chemical interactions, Cem. Concr. Res. 28 (7) (1998) 1037–1048.
[45] L. Armelao, A. Bassan, R. Bertoncello, G. Biscontin, S. Daolio, A. Glisenti, Silica glass interaction with calcium hydroxide: a surface chemistry approach, J. Cult. Herit. 1 (2000) 375–384.
[46] A.A. Kruger, The role of the surface of glass reinforcement fibers on their physical properties and performance in composites, in: S. Mindess, S.P. Shah (Eds.), Bonding in Cementitious Composites, Materials Research Society, Pittsburgh, 1988, pp. 181–186.
[47] F. Bonapasta, Cross-linking of poly(vinyl alcohol) chains by Ca ions in macro-defect-free cements, Chem. Mater. 14 (2002) 1016–1022.
[48] M.Y.A. Mollah, M. Kesmez, D.L. Cocke, An X-ray diffraction (XRD) and Fourier transform infrared spectroscopy (FT-IR) investigation of the long-term effect on the solidification/stabilization (S/S) of arsenic(V) in Portland cement type-V, Sci. Total Environ. 325 (2004) 255–262.
[49] JCPDS — International Centre for Diffraction Data, PCPDFWIN v. 2.2, 2001.
[50] J. Rottstegge, M. Wilhelm, H.W. Spiess, Solid state NMR investigations on the role of organic admixtures on the hydration of cement pastes, Cem. Concr. Compos. 28 (5) (2006, May) 417–426.
[51] M.Y.A. Mollah, W. Yu, R.E. Schennach, D.L. Cocke, A Fourier transform infrared spectroscopy of the early hydration of Portland cement and the influence of sodium lignosulfonate, Cem. Concr. Res. 30 (2) (2000) 267–273.
[52] M. Yousuf, A. Mollah, P. Palta, T.R. Hess, R.K. Vempati, D.L. Cocke, Chemical and physical effects of sodium lignosulfonate superplasticizer on the hydration of Portland cement and solidification/stabilization consequences, Cem. Concr. Res. 25 (3) (1995) 671–682.
[53] H.W. van der Marel, H. Beutelspacher, Atlas of Infrared Spectroscopy of Clay Minerals and their Admixtures, Elsevier Scientific Publishing Company, Amsterdam, 1976.
[54] V.C. Farmer, The Infrared Spectra of Minerals, Adlard & Son Ltd., London, 1974.